

# Shell Model and Mean-Field Description of Band Termination

M. Zalewski,<sup>1</sup> W. Satuła,<sup>1,2</sup> W. Nazarewicz,<sup>3,4,1</sup> G. Stoitchewa,<sup>5</sup> and H. Zduniczuk<sup>1</sup>

<sup>1</sup> *Institute of Theoretical Physics, University of Warsaw, ul. Hoża 69, 00-681 Warsaw, Poland*

<sup>2</sup> *Joint Institute for Heavy Ion Research, Oak Ridge National Laboratory, Oak Ridge, Tennessee 37831*

<sup>3</sup> *Department of Physics and Astronomy, University of Tennessee, Knoxville, Tennessee 37996*

<sup>4</sup> *Physics Division, Oak Ridge National Laboratory, Oak Ridge, Tennessee 37831*

<sup>5</sup> *Lawrence Livermore National Laboratory, P.O. Box 808, L-414, Livermore, California 94551*

(Dated: May 27, 2021)

We study nuclear high-spin states undergoing the transition to the fully stretched configuration with maximum angular momentum  $I_{max}$  within the space of valence nucleons. To this end, we perform a systematic theoretical analysis of non-fully-stretched  $I_{max} - 2$  and  $I_{max} - 1$   $f_{7/2}^n$  seniority isomers and  $d_{3/2}^{-1}f_{7/2}^{n+1}$  intruder states in the  $A \sim 44$  nuclei from the lower- $fp$  shell. We employ two theoretical approaches: (i) the density functional theory based on the cranked self-consistent Skyrme-Hartree-Fock method, and (ii) the nuclear shell model in the full  $sdfp$  configuration space allowing for 1p-1h cross-shell excitations. We emphasize the importance of restoration of broken angular momentum symmetry inherently obscuring the mean-field treatment of high-spin states. Overall good agreement with experimental data is obtained.

PACS numbers: 21.10.Pc, 21.10.Hw, 21.60.Cs, 21.60.Jz, 23.20.Lv, 27.40.+z

## I. INTRODUCTION

The phenomenon of band termination is a splendid manifestation of a competition between nuclear single-particle and collective motion. At low angular momenta, a rotational band is associated with a collective reorientation of a deformed nucleus in space, with many nucleons contributing coherently to the total spin. With increased rotational velocity, however, the Coriolis interaction causes nucleonic pairs to break, and the decoupled nucleons align their individual angular momenta. It often happens that breaking relatively few nucleonic pairs can give rise to a nuclear state with a fairly large spin. In the language of the nuclear shell model, of particular importance are the “seniority isomers” or “fully-aligned (or stretched, or optimal) states,” which carry the maximum angular momentum  $I_{max}$  within the space of valence nucleons.

The transition process from collective rotation at high spins to a single-particle picture at  $I_{max}$  is referred to as band termination [1]. Terminating bands are common in nuclei; they have been observed across the table of the nuclides (see recent reviews [2, 3]). The nature of the termination process strongly depends on the size of the valence space. For instance, if only several valence nucleons are present, the static nuclear deformation cannot develop and the collective effects have dynamic character. In this case,  $I_{max}$  can be generated by breaking very few nucleonic pairs, and the transition to the single-particle limit is rapid. On the other hand, for deformed nuclei having many valence nucleons, the transition to the non-collective regime is long and gradual, often involving many intermediate stages.

Theoretically, high-spin band terminations and fully aligned configurations are often discussed within the nuclear shell model (SM) and/or the self-consistent density functional theory (DFT). The nuclear shell model [4] can

be applied to nuclei with several valence nucleons outside the magic core. The effective Hamiltonian is exactly diagonalized in a subspace of many-body Slater determinants resulting in correlated wave functions that preserve angular momentum, parity, particle number, and - usually - isospin.

For medium-mass and heavy nuclei containing many valence nucleons, the tool of choice is the nuclear DFT [5]. Here, the nucleus is described in terms of one-body densities and currents representing distributions of nucleonic matter, spins, momentum, and kinetic energy, as well as their derivatives. The associated mean fields, obtained by means of the self-consistent Hartree-Fock (HF) procedure, are usually deformed, i.e., they spontaneously break the symmetries of the underlying Hamiltonian. In this way, many essential many-body correlations can be incorporated into a single product state [3, 5, 6]. However, the price paid for the simple intrinsic picture is high: the HF wave function is no longer an eigenstate of symmetry operators; hence, the transformation to the laboratory reference frame has to be carried out to restore broken symmetries.

The language in which the nucleus is pictured as a wave packet with anisotropic density/current distribution is particularly useful for the description of rotational motion within the cranking formalism. Here, the many-body Hamiltonian  $\hat{H}$  is replaced by a rotating Hamiltonian (Routhian),  $\hat{H}^\omega = \hat{H} - \omega \hat{J}_z$ , where the rotational frequency  $\omega$  is interpreted as a Lagrange multiplier determined from the angular momentum constraint. The resulting cranked HF method (CHF) can also be used to describe the so-called *non-collective* rotations, i.e., rotations around symmetry axis [2, 7]. The non-collective CHF technique applied in this work has proven to be a very efficient and accurate way to generate stretched solutions within a self-consistent framework.

In practice, most applications of nuclear DFT are

based on Skyrme energy density functionals optimized to various experimental data [5, 8]. Recently, such an approach was applied [9, 10] to fully-stretched, high-spin states associated with the  $[f_{7/2}^n]_{I_{max}}$  and  $[d_{3/2}^{-1}f_{7/2}^{n+1}]_{I_{max}}$  SM configurations ( $n$  denotes the number of valence particles outside the  $^{40}\text{Ca}$  core) of  $20 \leq Z \leq N \leq 24$ . These studies have demonstrated that those fully-aligned states have a fairly simple SM structure, and, therefore, they provide an excellent testing ground for both the time-odd densities and fields that appear in the mean-field description and for SM effective interactions. In particular, it was shown that the energy difference between the excitation energies of the terminating states,  $E([d_{3/2}^{-1}f_{7/2}^{n+1}]_{I_{max}}) - E([f_{7/2}^n]_{I_{max}})$ , is a sensitive probe of time-odd spin couplings and the strength of the spin-orbit term in the Skyrme functional [9], and that with properly modifying functionals, the nuclear DFT provides a description of the data for stretched states that is of similar quality as the fully correlated SM [10].

The aim of this study is to understand the nature of the  $[f_{7/2}^n]_{I_{max}-1}$  (Sec. III) and  $[d_{3/2}^{-1}f_{7/2}^{n+1}]_{I_{max}-1}$  (Sec. IV) configurations in the  $A \sim 44$  mass region. These  $I_{max} - 1$  states, usually referred to as unfavored-signature terminating states, can be obtained from fully-stretched configurations by signature-changing particle-hole (p-h) excitations. Consequently, their structure is sensitive to both shell structure and time-odd nuclear fields. We demonstrate that non-collective cranking may lead to a dramatic violation of rotational symmetry even for the cases when the nuclear shape is almost spherical. We also analyze in Sec. V the  $I_{max} - 2$  weakly collective states in terminating normal-parity and intruder structures. The associated correlation energy, mainly associated with quadrupole effects, is calculated to be large, around 2 MeV.

## II. THE MODELS

The details of DFT and SM frameworks applied in this study follow Ref. [10] in which the stretched configurations in the  $A \sim 44$  mass region have been successfully explained. The CHF calculations are carried out using the HFODD code of Ref. [11]. We employed the SLy4 [12] and SkO [13] Skyrme energy density functionals slightly modified along the prescription of Refs. [9]. Without going into detail, the modifications concern the coupling constants of  $\mathbf{s}^2$  and  $\mathbf{s} \cdot \Delta \mathbf{s}$  terms giving rise to the time-odd spin mean fields. This has been done by constraining the functionals to the empirical spin-isospin Landau parameters. In addition, the strength of the spin-orbit interaction has been reduced by 5% from the original SLy4 and SkO values. As discussed in Ref. [10], the DFT results for the  $T=0$  states in  $N=Z$  nuclei have to be corrected for the isospin breaking effects. Here we assume that the isospin correction weakly depends on angular momentum; hence, it has been neglected when discussing energy differences between high-spin states.

During the last decade, extensive SM calculations for the light  $fp$ -shell nuclei have been conducted using different SM interactions [14, 15, 16, 17, 18]. In most cases, SM reproduces well the excitation energies of normal-parity and intruder states, as well as transition rates. In general, the intruder  $d_{3/2}^{-1}f_{7/2}^{n+1}$  states are predicted and observed to be more collective than the  $f_{7/2}^n$  structures, i.e., the associated in-band  $E2$  rates are significantly greater within intruder bands. The SM results in this work are obtained using the code ANTOINE [19] in the *sdfp* configuration space limited to 1p-1h cross-shell excitation from the *sd* shell to the *fp* shell. In the *fp*-shell SM space we took the FPD6 interaction [20]. The remaining matrix elements are those of Ref. [21]. As compared to the earlier work [14], the mass scaling of the SM matrix elements was done here consistently, thus reducing the *sd* interaction channel by  $\sim 4\%$ .

## III. UNFAVORED-SIGNATURE TERMINATING $f_{7/2}^n$ STATES

We begin with  $[f_{7/2}^n]_{I_{max}-1}$  configurations in  $20 < Z \leq N \leq 24$  nuclei. Figure 1 displays the energy difference between the stretched  $I=I_{max}$  and the lowest  $I_{max} - 1$  states. It is gratifying to see a qualitative, and – in most cases – quantitative agreement between SM and experimental data.

Within the *naïve* non-collective cranking, the unfavored  $I_{max} - 1$  states can be obtained by either inverting the signature of a single proton ( $\pi$ ) or a single neutron ( $\nu$ ). The energies of those states,  $E_{I_{max}-1}^{(\text{CHF}, \pi)}$  and  $E_{I_{max}-1}^{(\text{CHF}, \nu)}$ , are displayed in Fig. 1 (top) with respect to the energy  $E_{I_{max}}^{(\text{CHF})}$  of the stretched configuration. It is seen that agreement between CHF and experiment is rather poor. In particular, the strong particle number variation in the energy difference is not reproduced by CHF. This discrepancy has its origin in the spontaneous violation of rotational invariance by the mean-field solutions, in spite of the fact that the underlying CHF states are almost spherical in all the considered cases. Indeed, since the cranking procedure only constrains an expectation value of the angular momentum projection, CHF states contain components with different angular momentum. In the case of unfavored  $I_{max} - 1$  states, two components are expected to dominate: spurious reorientation mode  $|I_{max}; I_{max} - 1\rangle$  and physical stretched configuration  $|I_{max} - 1; I_{max} - 1\rangle$ .

The appearance of spurious components in partially-aligned cranking configurations is well known [22]. A classic example is the cranking treatment of two identical nucleons in a spherical single- $j$  shell. While the stretched configuration with  $J_z=M=2j-1$  can be associated with the stretched state having  $I_{max}=2j-1$ , the cranked  $J_z=2j-2$  solution is simply a magnetic substate of  $I_{max}$  (the  $I_{max} - 1$  state does not exist in a  $j^2$  configuration as a result of the Pauli principle). In or-

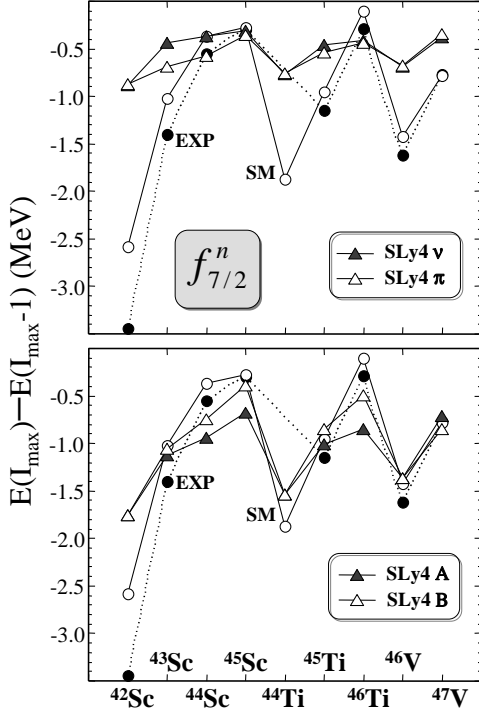


FIG. 1: The energy difference between  $I_{max}$  and  $I_{max} - 1$  states in  $f_{7/2}^n$  configurations in  $A \sim 44$  nuclei. Dots and circles mark experimental data and the SM results, respectively. Top: CHF-SLy4 results for unfavored signature terminating states corresponding to neutron (filled triangles) and proton (open triangles) signature inversion. Bottom: CHF-SLy4 results including the angular momentum correction calculated using prescription A (filled triangles) and B (open triangles).

der to remove spurious components, angular momentum needs to be restored. Since the number of  $M$ -scheme configurations around  $I_{max}$  is very limited, in our cranking analysis we resort to an approximate projection scheme. In the following, the adopted angular momentum restoration procedure is discussed for the case of  $^{43}\text{Sc}$ .

Due to a near-sphericity of the CHF solutions, single-particle (sp) states can be labeled using the angular momentum projection  $m$ . The optimal state  $|I_{max}; I_{max}\rangle$  can be viewed as a CHF vacuum around which p-h excitations are built. The  $|I_{max}; I_{max} - 1\rangle$  spurious state can be obtained by acting on the vacuum with the lowering operator  $\hat{I}_-$ . For  $^{43}\text{Sc}$ , which in a SM picture has one proton and two neutrons in a  $f_{7/2}$  shell,  $I_{max}^\pi = 19/2^-$  and the (unnormalized) spurious state can be written as

$$|I_{max}; I_{max} - 1\rangle = 2\sqrt{3}\hat{a}_{\nu 3/2}^\dagger \hat{a}_{\nu 5/2} |I_{max}; I_{max}\rangle + \sqrt{7}\hat{a}_{\pi 5/2}^\dagger \hat{a}_{\pi 7/2} |I_{max}; I_{max}\rangle \equiv a|\nu\rangle + b|\pi\rangle, \quad (1)$$

TABLE I: Maximum spin states  $I_{max}^\pi$  and squared unnormalized expansion amplitudes for  $f_{7/2}^n$  and  $d_{3/2}^{-1}f_{7/2}^{n+1}$  configurations in  $A \sim 44$  nuclei. In the latter case only  $N \neq Z$  nuclei are considered.

	$I_{max}$	$a^2$	$b^2$	$I_{max}$	$a^2$	$b^2$	$c^2$
$^{42}\text{Ca}$				$11^-$	12	7	3
$^{44}\text{Ca}$				$13^-$	16	7	3
$^{42}\text{Sc}$	$7^+$	1	1				
$^{43}\text{Sc}$	$19/2^-$	12	7	$27/2^+$	12	12	3
$^{44}\text{Sc}$	$11^+$	15	7	$15^-$	15	12	3
$^{45}\text{Sc}$	$23/2^-$	16	7	$31/2^+$	16	12	3
$^{44}\text{Ti}$	$12^+$	1	1				
$^{45}\text{Ti}$	$27/2^-$	15	12	$33/2^+$	15	15	3
$^{46}\text{Ti}$	$14^+$	16	12	$17^-$	16	15	3
$^{46}\text{V}$	$15^+$	1	1				
$^{47}\text{V}$	$31/2^-$	16	15	$35/2^+$	16	16	3

where  $\hat{a}_{\tau m}^\dagger$  ( $\tau = \pi$  or  $\nu$ ) represents a particle in the  $f_{7/2}$  shell carrying magnetic quantum number  $m$ . By assuming that the valence coupling scheme (1) can be extended to the CHF case, the  $|I_{max}; I_{max} - 1\rangle$  state can be represented as a unique combination of CHF solutions  $|\nu\rangle$  and  $|\pi\rangle$  corresponding to the lowest neutron and proton p-h signature-changing excitations.

The mixing coefficients  $a$  and  $b$  introduced in Eq. (1) for  $^{43}\text{Sc}$  can be calculated in a similar manner for any nucleus. They are displayed in Table I. Assuming that contributions from other shells are small, the physical state  $|I_{max} - 1; I_{max} - 1\rangle$  can be represented by the orthogonal combination:

$$|I_{max} - 1; I_{max} - 1\rangle = -b|\nu\rangle + a|\pi\rangle. \quad (2)$$

This  $2 \times 2$  configuration mixing can be dealt with using two slightly different methods. In the first variant (called A in the following), one requires that the spurious solution is degenerate with respect to the CHF optimal state having energy  $E_{I_{max}}^{(\text{CHF})}$ . This assumption leads to a simple expression for the energy of the unfavored-signature terminating state

$$E_{I_{max}-1}^{(\text{CHF}, A)} = E_{I_{max}-1}^{(\text{CHF}, \pi)} + E_{I_{max}-1}^{(\text{CHF}, \nu)} - E_{I_{max}}^{(\text{CHF})}. \quad (3)$$

In the second variant (called B), the mixing coefficients are taken directly from Table I and the corresponding energy can be written as

$$E_{I_{max}-1}^{(\text{CHF}, B)} = \frac{a^2 E_{I_{max}-1}^{(\text{CHF}, \pi)} - b^2 E_{I_{max}-1}^{(\text{CHF}, \nu)}}{a^2 - b^2}. \quad (4)$$

Note that this method cannot be applied to  $N=Z$  nuclei where  $a^2=b^2$ . Moreover, method B does not guarantee that the energy of the spurious state is degenerate with the optimal state.

The energy differences between  $I_{max}$  and  $I_{max}-1$  states obtained in variants A and B are displayed in the lower panel of Fig. 1. It is seen that the effect of

symmetry restoration is large. In particular, the energies corrected for the angular momentum mixing follow fairly accurately experiment and SM. Moreover, methods A and B give fairly similar results, although method B is slightly closer to the data. Similar results were also obtained in the CHF-SkO variant.

#### IV. UNFAVORED-SIGNATURE TERMINATING $d_{3/2}^{-1}f_{7/2}^{n+1}$ STATES

We now consider the  $[d_{3/2}^{-1}f_{7/2}^{n+1}]_{I_{max}-1}$  intruder configurations. Let us recall that in this case the  $[d_{3/2}^{-1}f_{7/2}^{n+1}]_{I_{max}}$  configurations are uniquely defined only for  $N \neq Z$  nuclei. Indeed, as discussed in Ref. [10], the CHF solutions for  $N=Z$  systems violate isobaric symmetry and can no longer serve as reference states. Hence, we shall limit our considerations to  $20 \leq Z < N \leq 24$  nuclei. Moreover, in the following, we will consider only configurations involving 1p-1h proton excitation across the  $Z=20$  gap. The latter assumption concerns the  $N-Z=1$  nuclei in which the neutron cross-shell excitations can also give rise to aligned  $I_{max}-1$  states. It is worth mentioning that the 1p-1h neutron excitations in  $N-Z=1$  nuclei are higher than the lowest 1p-1h proton excitations. Moreover, they do not mix at the level of CHF, leading to a severe isospin symmetry violation. Restoration of the isospin symmetry for these cases is, however, beyond the scope of this work.

Under these assumptions, within the non-collective cranked CHF picture, there are three obvious ways of changing the signature quantum number of an intruder state. Namely, one can invert the signature of a single  $f_{7/2}$  proton ( $|\pi\rangle$ ), a single  $f_{7/2}$  neutron ( $|\nu\rangle$ ), or a proton  $d_{3/2}$  hole ( $|\bar{\pi}\rangle$ ). In this case, SM yields two independent  $(I_{max}-1)_i$  ( $i=1,2$ ) low-lying solutions. In CHF, both these solutions are polluted by the presence of spurious  $|I_{max}; I_{max}-1\rangle$  components.

Since the CHF solutions for the aligned intruder states are nearly spherical, we can employ the same technique as proposed earlier for the  $f_{7/2}^n$  stretched states to approximately restore the rotational invariance. The only difference is that in addition to active  $f_{7/2}$  particles, one has to consider active  $d_{3/2}$  proton holes (denoted as  $\bar{\pi}$  in the following). As usual, the  $|I_{max}, I_{max}-1\rangle$  is obtained by acting with  $\hat{I}_-$  on the  $|I_{max}, I_{max}\rangle$  CHF vacuum. For the representative case of  $^{42}\text{Ca}$  one obtains:

$$\begin{aligned} |I_{max}, I_{max}-1\rangle &= \sqrt{12} \hat{a}_{\nu 3/2}^\dagger \hat{a}_{\nu 5/2} |I_{max}, I_{max}\rangle \\ &+ \sqrt{7} \hat{a}_{\pi 5/2}^\dagger \hat{a}_{\pi 7/2} |I_{max}, I_{max}\rangle \\ &+ \sqrt{3} \hat{a}_{\bar{\pi} 1/2}^\dagger \hat{a}_{\bar{\pi} 3/2} |I_{max}, I_{max}\rangle \\ &\equiv a|\nu\rangle + b|\pi\rangle + c|\bar{\pi}\rangle. \end{aligned} \quad (5)$$

Similar calculations can be carried out for all  $N \neq Z$  nuclei. The resulting mixing coefficients are collected in Table I.

The intruder case represents a  $3 \times 3$  mixing problem. Two different analytical approximate projection techniques have been developed [23]. In the first method (called A), we assume real mixing matrix elements and require the eigenvector  $(a, b, c)$  of Eq. (5) and Table I to correspond to zero energy mode relative to the CHF energy  $E_{I_{max}}^{(\text{CHF})}$  of the optimal solution. By introducing  $e_\alpha = E_{I_{max}-1}^{(\text{CHF}, \alpha)} - E_{I_{max}}^{(\text{CHF})}$ , where  $\alpha = \nu$  (or 1),  $\pi$  (or 2), and  $\bar{\pi}$  (or 3), the energies of physical solutions relative to the CHF optimal state  $E_{I_{max}}^{(\text{CHF})}$  are:

$$\lambda_\pm = \frac{1}{2} \left( \sum_i e_i \pm \sqrt{(\sum_i e_i)^2 - 4Z} \right), \quad (6)$$

where

$$Z = \sum_{i < j} (e_i e_j - |V_{ij}|^2) \quad (7)$$

and

$$\begin{aligned} V_{12} &= \frac{-e_1 a^2 - e_2 b^2 + e_3 c^2}{2ab}, \\ V_{13} &= \frac{-e_1 a^2 + e_2 b^2 - e_3 c^2}{2ac}, \\ V_{23} &= \frac{e_1 a^2 - e_2 b^2 - e_3 c^2}{2bc}. \end{aligned} \quad (8)$$

In the second method (called B), we admit complex mixing amplitudes. In this case we set the spurious mode to zero but do not require the corresponding eigenvector to be equal  $(a, b, c)$ . This procedure leads to exactly the same set of formulas (6)-(7) as above but with  $V_{\alpha\beta} = \sqrt{e_\alpha e_\beta}$  (see Ref. [23] for further details).

The SM and CHF results corresponding to the lowest  $(I_{max}-1)_1$  states are shown in Fig. 2. The agreement between SM and experiment is again excellent, except for the  $T=1/2$  nuclei  $^{43}\text{Sc}$  and  $^{47}\text{V}$  where theory overestimates the energy difference between  $I_{max}$  and  $I_{max}-1$  intruder states. In order to understand this apparent discrepancy, Fig. 2 also shows the SM results for excited  $(I_{max}-1)_2$  states in  $T=1/2$  nuclei. It turns out that for  $^{47}\text{V}$  the calculated  $33/2_1^+$  level has a neutron intruder character, while it is the second  $33/2_2^+$  state in which the proton intruder configuration dominates. For  $^{45}\text{Ti}$ , the calculated  $31/2_{1,2}^+$  states have a mixed proton-neutron intruder character with a slight preference for a proton configuration, and the same is true for the  $25/2_{1,2}^+$  states in  $^{43}\text{Sc}$ . Clearly, the energetics of  $(I_{max}-1)_1$  and  $(I_{max}-1)_2$  states in  $T=1/2$  nuclei strongly depends on the mixing between proton and neutron intruder states, i.e., the isospin dependence of the cross-shell  $sd \leftrightarrow fp$  interaction.

The CHF calculations displayed in Fig. 2 were carried out for the SLy4 (top) and SkO (bottom) Skyrme parameterizations. It is interesting to see that predictions for  $d_{3/2}^{-1}f_{7/2}^{n+1}$  intruder states strongly depend on the energy density functional. The mean empirical value of

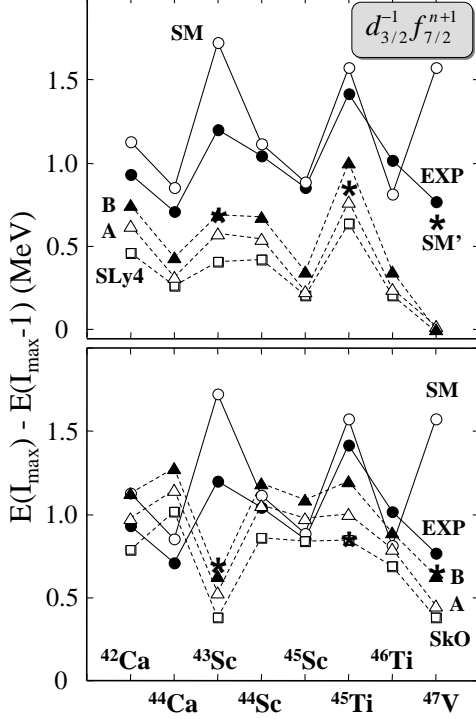


FIG. 2: The energy difference between  $I_{max}$  and  $(I_{max} - 1)_1$  states in  $d_{3/2}^{-1} f_{7/2}^{n+1}$  configurations in  $A \sim 44$  nuclei. Dots and circles mark experimental data and the SM results, respectively. The asterisk symbols (SM') show the SM results for the  $(I_{max} - 1)_2$  states in  $T=1/2$  Sc, Ti, and V isotopes. The CHF results with the SLy4 and SkO functionals are shown in the upper and lower panel, respectively. The lowest cranked solution ( $|\bar{\pi}\rangle$ ) is marked by squares while open (filled) triangles mark the results obtained within the approximate angular momentum projection A(B) are marked with open (filled) triangles.

$\Delta E \equiv E(I_{max}) - E_1(I_{max} - 1)$ , averaged over all nuclei considered, is  $\overline{\Delta E}_{EXP} \approx 0.990$  keV. For the lowest CHF solutions corresponding to  $\bar{\pi}$ -type configurations (marked by squares in the figures), the calculations yield  $\overline{\Delta E}_{SLy4} \approx 0.330$  keV and  $\overline{\Delta E}_{SkO} \approx 0.730$  keV. The calculated corrections are of similar size for both Skyrme functionals, and in all cases they improve the agreement with the data. Within method A, the CHF curves are shifted up, on the average, by  $\delta\overline{\Delta E}_{SLy4} \approx 0.090$  keV and  $\delta\overline{\Delta E}_{SkO} \approx 0.140$  keV. The corrections obtained in variant B are  $\delta\overline{\Delta E}_{SLy4} \approx 0.210$  keV and  $\delta\overline{\Delta E}_{SkO} \approx 0.270$  keV.

In variant B, the average splitting calculated in CHF-SkO is fairly close to the experimental value,  $\overline{\Delta E}_{SkO} \approx \overline{\Delta E}_{EXP} \approx 1$  MeV. However, clear discrepancies in the isotopic and isotonic dependence are seen. Applying pro-

jection method B to CHF-SLy4 yields an almost constant offset of  $\Delta E_{EXP} - \overline{\Delta E}_{SLy4} \sim 0.450$  keV. Indeed, by shifting the theoretical results up by  $\sim 0.450$  keV, one reproduces surprisingly well the empirical isotopic and isotonic dependence, including the cases of  $^{43}\text{Sc}$  and  $^{47}\text{V}$ . It is important to point out that both methods A and B are free from adjustable parameters. In both cases we have simplified the picture by limiting the size of the configuration space to three states, and in both cases we have forced the spurious mode to have zero energy.

## V. FAVORITE SIGNATURE TERMINATING $I_{max} - 2$ STATES

In the standard picture of band termination, the  $I_{max} - 2$  configurations contain some quadrupole collectivity. That is, these states have small quadrupole deformations that give rise to a small collective rotational component in the wave function. One can therefore expect that the energy difference between  $I_{max}$  and  $I_{max} - 2$  states should mainly depend on time-even nuclear multipole fields associated with the nuclear deformability. The energy of the last quadrupole transition within the terminating sequence,  $\Delta E_2 \equiv E(I_{max}) - E(I_{max} - 2)$ , is shown in Fig. 3 for both  $f_{7/2}^n$  (top) and  $d_{3/2}^{-1} f_{7/2}^{n+1}$  (bottom) structures. The agreement between SM and experiment is excellent. In  $^{42}\text{Ca}$ ,  $^{43,44}\text{Sc}$ , and  $^{45}\text{Ti}$ , the  $B(E2)$  rates for the  $I_{max} \rightarrow (I_{max} - 2)_2$  transitions are significantly larger than those for the yrast  $I_{max} \rightarrow (I_{max} - 2)_1$  transitions. In these cases, the quadrupole strength is fragmented and the band structures cannot be easily identified. It is interesting to see that  $\Delta E_2$  for the  $f_{7/2}^n$  configurations is significantly smaller (and sometimes even negative) as compared to the  $d_{3/2}^{-1} f_{7/2}^{n+1}$  values. This is consistent with the fact that the quadrupole polarization in the intruder states is significantly greater than in the  $f_{7/2}^n$  structures.

The mean p-h  $\Delta J_z = -2$  excitation energy calculated in HF-SLy4 lies  $\sim 2$  MeV below the data. By performing self-consistent cranking, one arrives at a slightly collective solution that, on the average, is not too far from experiment. For the weakly collective, normal-parity structures, the CHF theory poorly reproduces the particle-number dependence. The situation is significantly improved in the more collective intruder states where the mean-field theory (both in CHF-SLy4 and CHF-SkO variants) performs much better. Here, the energy gain due to deformation can be as large as  $\sim 2$  MeV. Of course, a big part of the remaining discrepancy between CHF results and experiment is due to angular momentum violation in the  $I_{max} - 2$  states. Unfortunately, for those states, the approximate methods of restoring rotational invariance discussed in the previous sections do not apply because of many states involved (i.e., pronounced configuration mixing).

## VI. CONCLUSIONS

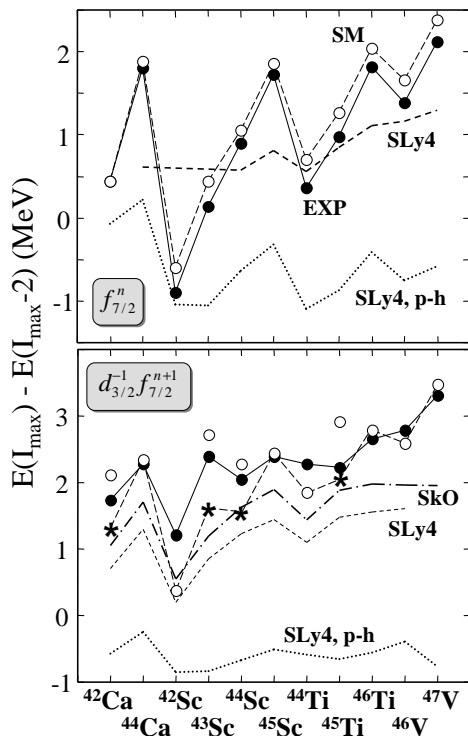


FIG. 3: The transition energy between  $I_{max}$  and  $(I_{max} - 2)_1$  states in  $f_{7/2}^n$  (top) and  $d_{3/2}^{-1} f_{7/2}^{n+1}$  (bottom) configurations in  $A \sim 44$  nuclei. Dots and circles mark experimental data and the SM results, respectively. The intruder  $(I_{max} - 2)_2$  states in  $^{42}\text{Ca}$ ,  $^{43,44}\text{Sc}$ , and  $^{45}\text{Ti}$  are shown by asterisks. In those nuclei, the  $B(E2)$  rates for the  $I_{max} \rightarrow (I_{max} - 2)_2$  transitions are significantly larger than those for the yrast  $I_{max} \rightarrow (I_{max} - 2)_1$  transitions. The CHF-SLy4 results are marked by a short-dashed line. The corresponding average particle-hole excitation energy is shown by a dotted line. For comparison, the CHF-SkO results (dash-dotted line) are given in the bottom panel.

In this work we performed a theoretical analysis of optimal  $I_{max}$  states and non-fully-stretched  $I_{max} - 2$  and  $I_{max} - 1$  states in the  $A \sim 44$  nuclei from the lower- $fp$  shell. Overall, the level of agreement between SM results and experimental data for  $f_{7/2}^n$  seniority isomers and  $d_{3/2}^{-1} f_{7/2}^{n+1}$  intruder states is excellent. We have shown that CHF solutions for unfavored-signature terminating states are affected by dramatic violation of rotational symmetry even if the shape of nuclei under consideration is almost spherical. Approximate methods of restoring rotational invariance in  $I_{max} - 1$  configurations have been proposed. The energy corrections due to angular momentum projection can be significant, and their inclusion improve agreement with the data. Finally, we investigated the weakly collective  $I_{max} - 2$  members of terminating structures. The correlation energy in these states, mainly of a quadrupole nature, is fairly large. While for nearly-spherical high-spin  $f_{7/2}^n$  states the CHF method gives only a rough estimate of the energy splitting between  $I_{max} - 2$  and  $I_{max}$  states, the agreement is more quantitative for intruder configurations.

## Acknowledgments

This work was supported in part by the U.S. Department of Energy under Contract Nos. DE-FG02-96ER40963 (University of Tennessee), DE-AC05-00OR22725 with UT-Battelle, LLC (Oak Ridge National Laboratory), DE-FG05-87ER40361 (Joint Institute for Heavy Ion Research), W-7405-Eng-48 with University of California (Lawrence Livermore National Laboratory); by the Polish Committee for Scientific Research (KBN) under contract No. 1 P03B 059 27; and by the Foundation for Polish Science (FNP).

- 
- [1] A. Bohr and B.R. Mottelson, *Nuclear Structure*, Vol. II (W.A. Benjamin, New York, 1975).
  - [2] A.V. Afanasjev, D.B. Fossan, G.J. Lane, and I. Ragnarsson, *Phys. Rep.* **322**, 1 (1999).
  - [3] W. Satuła and R. Wyss, *Rep. Prog. Phys.* **68**, 131 (2005).
  - [4] E. Caurier, G. Martínez-Pinedo, F. Nowacki, A. Poves and A.P. Zuker, *Rev. Mod. Phys.* **77**, 427 (2005).
  - [5] M. Bender, P.-H. Heenen, and P.-G. Reinhard, *Rev. Mod. Phys.* **75**, 121 (2003).
  - [6] P. Ring and P. Schuck, *The Nuclear Many Body Problem* (Springer-Verlag, New York, 1980).
  - [7] Z. Szymański, *Fast Nuclear Rotation*, (Clarendon Press, Oxford 1983).
  - [8] M.V. Stoitsov, J. Dobaczewski, W. Nazarewicz, and P. Borycki, *Int. J. Mass Spectrometry* **251**, 243 (2006).
  - [9] H. Zduńczuk, W. Satuła, and R.A. Wyss, *Phys. Rev. C* **71**, 024305 (2005); *Int. J. Mod. Phys. E* **14**, 451 (2005).
  - [10] G. Stoitchewa, W. Satuła, W. Nazarewicz, D.J. Dean, M. Zalewski, and H. Zduńczuk, *Phys. Rev. C* **73**, 061304(R) (2006).
  - [11] J. Dobaczewski and J. Dudek, *Comput. Phys. Comm.* **131**, 164 (2000); J. Dobaczewski and P. Olbratowski, *ibid.* **158**, 158 (2004); HFODD User's Guide nucl-th/0501008.
  - [12] E. Chabanat, P. Bonche, P. Haensel, J. Meyer, and F. Schaeffer, *Nucl. Phys. A* **627**, 710 (1997) ; *A* **635**, 231 (1998).
  - [13] P.-G. Reinhard, D.J. Dean, W. Nazarewicz, J. Dobaczewski, J.A. Maruhn, and M.R. Strayer, *Phys. Rev. C* **60**, 014316 (1999).

- [14] P. Bednarczyk, J.Styczeń, R. Broda, M. Lach, W. Męczyński, W. Nazarewicz, W.E. Ormand, W. Satuła, D. Bazzacco, F. Brandolini, G. de Angelis, S. Lunardi, L. Müller, N. Medina, C. Petrache, C. Rossi-Alvarez, F. Scarlassara, G.F. Segato, C. Signorini, and F. Soramel, *Phys. Lett. B* **393**, 285 (1997).
- [15] A. Poves and J.S. Solano, *Phys. Rev. C* **58**, 179 (1998).
- [16] F. Brandolini, N.H. Medina, R.V. Ribas, S.M. Lenzi, A. Gadea, C.A. Ur, D. Bazzacco, R. Menegazzo, P. Pavan, C. Rossi-Alvarez, A. Algorta-Pineda, G. de Angelis, M. De Poli, E. Farnea, N. Marginean, T. Martinez, D.R. Napoli, M. Ionescu-Bujor, A. Iordachescu, J.A. Cameron, S. Kasemann, I. Schneider, J.M. Espino, and J. Sanchez-Solano, *Nucl. Phys. A* **693**, 517 (2001); F. Brandolini and C.A. Ur, *Phys. Rev. C* **71**, 054316 (2005).
- [17] M. Hasegawa, K. Kaneko, and S. Tazaki, *Nucl. Phys. A* **674**, 411 (2000).
- [18] A. Juodagalvis, I. Ragnarsson, and S. Åberg, *Phys. Rev. C* **73**, 044327 (2006).
- [19] E. Caurier, J.L. Egido, G. Martinez-Pinedo, A. Poves, J. Retamosa, L.M. Robledo, and A.P. Zuker, *Phys. Rev. Lett.* **75**, 2466 (1995).
- [20] W.A. Richter, M.G. Vandermerwe, R.E. Julies, and B.A. Brown, *Nucl. Phys. A* **523**, 325 (1991).
- [21] E.K. Warburton, J.A. Becker, and B.A. Brown, *Phys. Rev. C* **41**, 1147 (1990).
- [22] A. Åberg, T. Døssing, and K. Neergård, *Nucl. Phys. A* **443**, 91 (1985).
- [23] M. Zalewski and W. Satuła, *Int. J. Mod. Phys. E* (2006), in press.